JOURNAL OF MATERIALS SCIENCE 20 (1985) 3842–3852

A study of craze deformation in the fatigue fracture of polymethylmethacrylate

Y. IMAI,* I. M. WARD
Department of Physics, University of Leeds, Leeds, UK

Continuous measurements of the craze contour have been undertaken for fatigue crack propagation in polymethylmethacrylate. The craze contour was determined by an interference fringe method, using equipment specially constructed for continuous load cycling, mounted on the stage of an optical microscope. It was found that there was a very great variation in the size of the craze for a fixed loading programme, although the crack growth rate showed a good correlation with the applied stress intensity range. A general result is that the craze length in fatigue was found to be greater than that for continuous crack propagation under simple fracture. This result suggested that it would be instructive to examine an extension of the Dugdale line-zone model, where the craze stress is not assumed to be constant along the length of the craze. It is shown that this modified line-zone model can provide some understanding of the observed results for craze deformation in fatigue.

1. Introduction

It is well known that the brittle fracture of glassy polymers is usually associated with the formation and fracture of a craze zone at the crack tip. The size and geometry of the craze relate to the state of stress at the crack tip, and hence provide information regarding the fracture mechanism. In a number of glassy polymers the craze zone can be conveniently studied by observing the optical interference fringes in reflected light [1–9]. These fringes arise due to the difference in refractive indices between bulk polymer and the craze, and can be used to provide a direct determination of the craze profile.

It has been found that the craze geometry can be described to a reasonable approximation, and sometimes a very good approximation, by the Dugdale plastic zone model [10]. This assumes a line-zone of yielding ahead of the crack tip and a constant yield stress, or "craze stress" in the case of a glassy polymer, where the craze stress is not identical to the bulk yield stress. Although there have been some doubts [6] regarding the applicability of the Dugdale zone model, it has proved a valuable starting point for the studies of brittle fracture in several glassy polymers [1, 2], and has also been applied to fatigue fracture [3, 4] with some success. However, in the case of discontinuous fatigue crack growth, which has been studied recently [8, 11], there are indications that the craze and crack growth may not be explained adequately by the simple Dugdale model.

In this paper, results are presented for the continuous monitoring of the craze geometry at the crack tip during loading and unloading of polymethylmethacrylate (PMMA) in low-frequency fatigue fracture. Examination of the craze shapes observed has led us to elaborate the simple Dugdale line-zone model, and to consider the effect of a stress distribution along the craze. In addition, we have considered the importance

Present address: Department of Mechanical Engineering, Nagasaki University, Nagasaki 852, Japan.

0022–2461/85 $03.00 + .12

of the initial thickness of the bulk material which forms the craze.

2. Experimental procedure

2.1. Crack growth rate measurement

A special loading device for fatigue loading was designed and fixed on the X–Y stage of the microscope as shown in Fig. 1. The load is applied by a cam-lever system A. The shape of the cam determines the loading waveform, and the position of the cam along the lever gives the displacement. The load is therefore determined by the displacement, and by the stiffness of the load cell and the specimen. The applied load is measured to an accuracy of ± 0.1 N by a leaf-spring type of load cell B which is installed between the specimen lower grip and the lever. The cam is driven by a synchronous electric motor C to obtain a precise loading rate. The crack length is easily measured with the microscope stage scale by maintaining the crack front in the centre of the field of view. The material used was commercial-grade PMMA manufactured by ICI Ltd under the trade name Perspex.

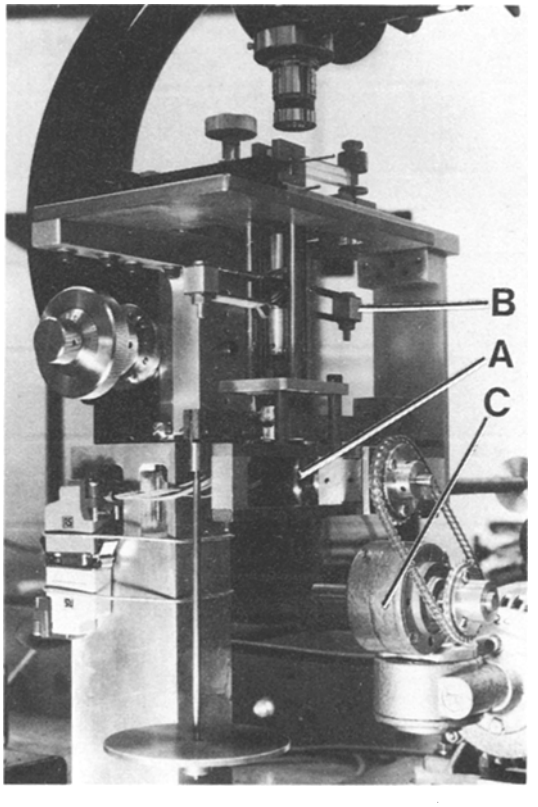

Figure 1 Fatigue loading device installed on a microscope stage. (A) cam–lever system, (B) load cell, (C) motor.

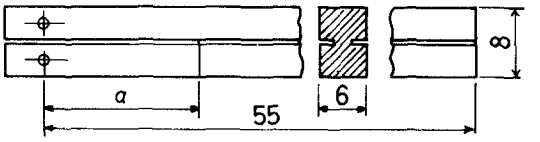

Figure 2 Double cantilever beam type specimen. Dimensions in millimetres. Crack length a is measured as shown.

Double cantilever beam specimens as shown in Fig. 2 were used. In order to achieve flat and straight front cracks, side grooves of depth 2 mm were machined on the specimen. The effective thickness B_e derived from the compliance calibration for several specimens was shown to be given in terms of total thickness B and net thickness B_n at a grooved section as

$$B_e = (BB_n)^{\frac{1}{2}}$$

to a very good approximation. The applied stress intensity was calculated from the formula for the double cantilever beam [12]

$$K = (12)^{\frac{1}{2}} \frac{P}{H^{\frac{1}{2}} B_e} \left(\frac{a}{H} + 0.7 \right)$$

where P is the applied load, H half the specimen height, and a the crack length measured from the loading line, as shown in Fig. 2.

The initial crack was introduced by tapping a razor blade into the machined crack, but no measurements were undertaken until the fatigue crack had grown by more than 5 mm. Throughout the experiment, K_{min} was kept less than 10% of K_{max}. The cyclic rate 0.1 Hz was used for crack growth measurement.

Three different loading waveforms were used. These are shown in Fig. 3 and have been designated *symmetric triangular*, *assymmetric triangular* and *trapezoidal*.

2.2. Craze contour measurement

The usual optical interference method was employed to measure the craze contour. In order to record the successive variation of contour during loading, the cyclic rate was reduced to 0.025 Hz. After at least 0.1 mm crack growth under the same loading conditions, optical interference patterns from the craze were photographed in several successive cycles. These patterns were traced by a microdensitometer giving a final magnification in craze length of

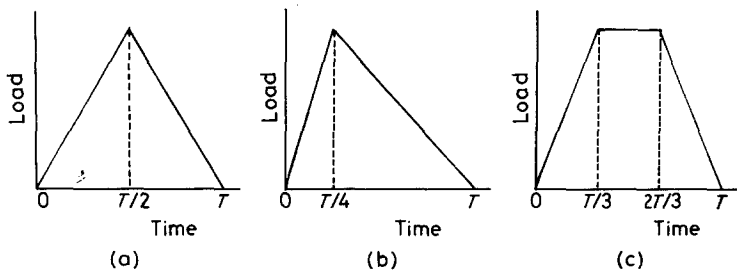

Figure 3 Loading waveforms: (a) symmetric triangular, (b) asymmetric triangular, (c) trapezoidal shape.

6250. It is estimated that the craze length could be determined to $\pm 0.5\,\mu$m.

The refractive index of craze μ was assumed to relate to the extension ratio λ as

$$\frac{\mu^2 - 1}{\mu^2 + 2} = \left(\frac{\mu_0^2 - 1}{\mu_0^2 + 2}\right)\frac{1}{\lambda}$$

where μ_0 is the refractive index of bulk material ($= 1.49$) and λ is the actual strain of the craze fibril from the bulk state [2]. Assuming that λ varies linearly with load from a relaxed value of 1.5 at the minimum load to 4.5 at the maximum load, the refractive index μ at any load level can then be obtained.

3. Results and discussion

3.1. Crack growth rate

Crack growth rate measurements were undertaken for a range of ΔK from about 0.4 to 0.9 MN m$^{-3/2}$. Within the fairly considerable scatter of the results, no significant differences were observed between growth rates for the different loading waveforms. Fig. 4 shows the results for the symmetric triangular waveform, on a log–log plot. As anticipated from previous work, for example by Hertzberg and co-workers [11] and from previous studies in our laboratories [13], there is an approximately linear relationship on this plot between crack growth rate and ΔK. Closer examination does, however, reveal a minor transition at about 0.7 MN m$^{-3/2}$. Up to this ΔK level the crack front remains fairly straight, and clear interference patterns can be observed. However, at 0.7 MN m$^{-3/2}$ it can be seen that some part of the crack front becomes rough, and this rough region then spreads across the crack front as the crack grows. In this region the crack growth rate remains approximately constant as ΔK increases. With further increase in ΔK the crack growth rate again increases with ΔK at about the same rate as for low ΔK. At the same time the crack front remains quite rough. This transition from smooth-surface crack growth to rough-surface crack growth may correspond to the appearance of plateaux in previous plots [9] of growth rate against ΔK.

The rough-surface crack growth mode can only be changed to a smooth-surface mode by reducing ΔK very substantially, or sometimes by increasing ΔK to the point where the crack produces in each loading cycle an entirely new craze beyond the rough crack growth region. It should perhaps be pointed out that these rough- and smooth-surface crack growth modes were also observed in the case of fracture [1].

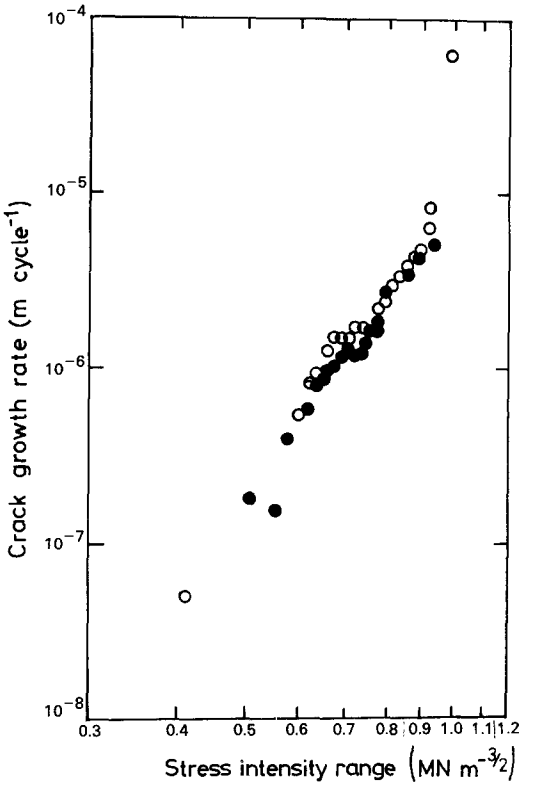

Figure 4 Crack growth rate against stress intensity range for PMMA. Symmetric triangular waveform, 0.1 Hz. Full circles and open circles show data for two specimens tested under identical conditions.

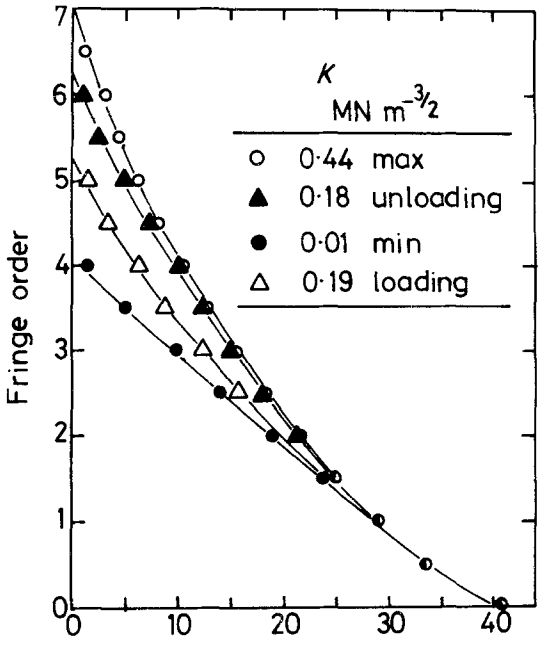

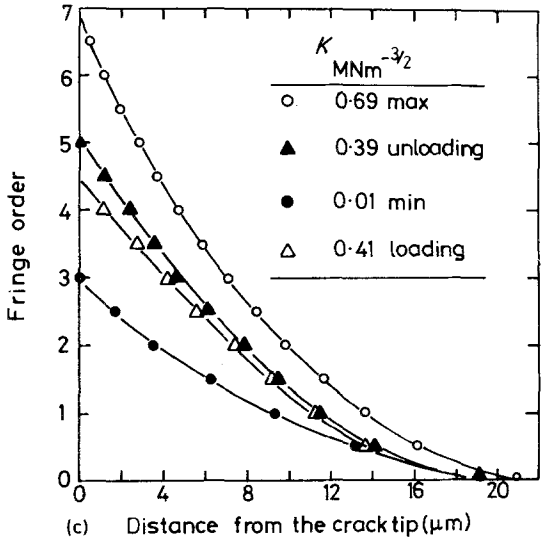

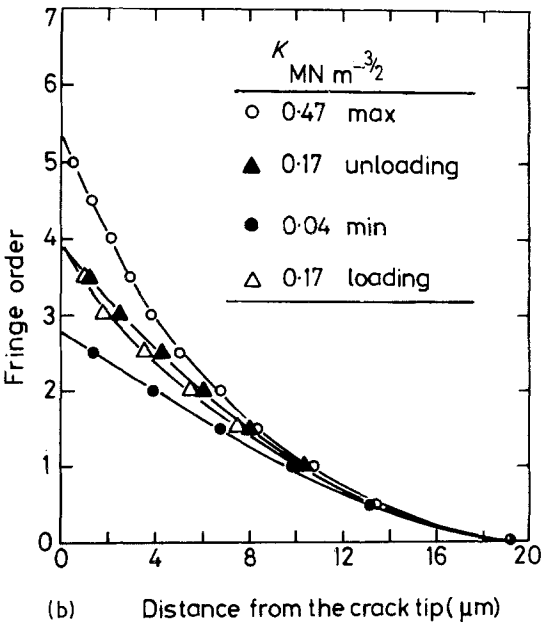

Figure 5 Measured craze contours at various loading levels during one complete fatigue cycle. Symmetric triangular waveform, 0.025 Hz: (a) $K_{max} = 0.44\,MN\,m^{-3/2}$, (b) $K_{max} = 0.47\,MN\,m^{-3/2}$, (c) $K_{max} = 0.69\,MN\,m^{-3/2}$.

3.2. Optical examination of crazes: general features

Photographs were obtained of the craze during loading and unloading, for a number of levels of ΔK. A typical set of results is shown in Fig. 5. It can be seen that the craze dimensions stabilize to a standard shape, varying between the lower bound for K_{min} and the upper bound for K_{max}. The actual overall shape approximates to that of a Dugdale plastic zone, as noted extensively for fracture in previous work, and more recently for fatigue [13].

There are, however, two features of the crazes in fatigue which we consider are importantly different from those observed in fracture. Firstly, very large differences in craze length were observed for identical loading conditions, i.e. ΔK and loading waveform. The craze contours were always very similar, and the maximum displacement at the crack tip also varied so that the crazes were of different overall size. Secondly, the fatigue crazes always appeared to be much larger than those observed for continuous crack growth. These results, obtained *in situ* during fatigue cycling, confirm completely the conclusions drawn in previous work [13] based on measurements on crazes cut from specimens after the cessation of fatigue loading.

It is of interest to examine some typical results for the fringe patterns which illustrate these two features, and which serve to introduce the approach we have adopted to the interpretation of fatigue crazes. In Figs. 5a and b, two craze contours are presented for loading and unloading conditions at comparatively low K_{max}. Although the K_{max} values are very close, the craze length varies from 20 to 40 μm and there is a similar change in the opening displacement at the craze tip, as indicated by the fringe order. It

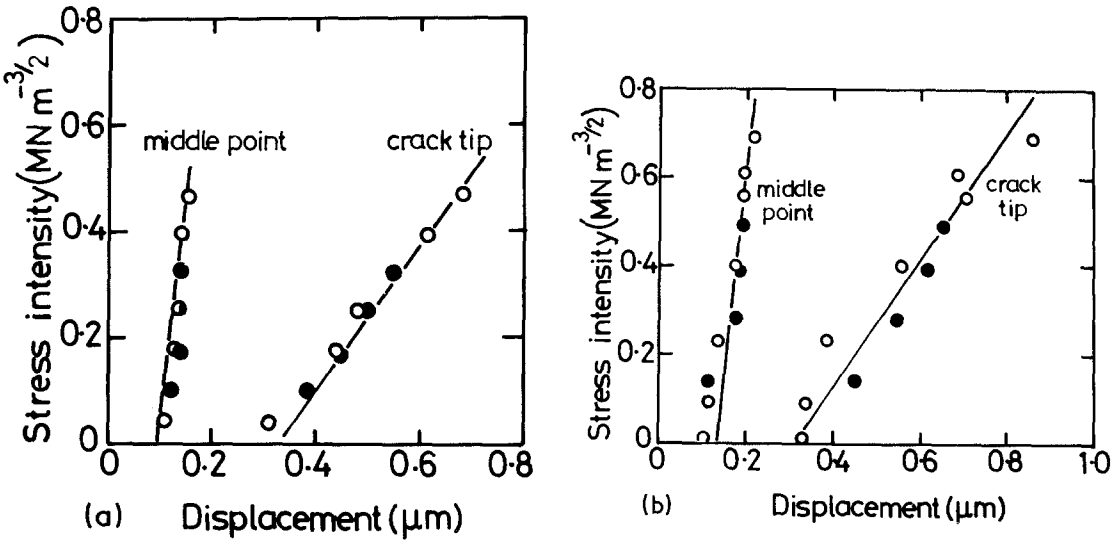

Figure 6 Variation of craze thickness at the crack tip and at the middle point of the craze length as a function of the applied stress intensity. Symmetric triangular waveform, 0.025 Hz: (a) $\Delta K = 0.43\,\mathrm{MN\,m^{-3/2}}$, craze length $R = 19\,\mu\mathrm{m}$; (b) $\Delta K = 0.68\,\mathrm{MN\,m^{-3/2}}$, craze length $R = 19\,\mu\mathrm{m}$.

is clear that the extension of the craze on loading is not uniform over the length of the craze and, especially in the case of the longer craze, there would appear to be very little extension of the craze in the region near the craze tip. This result is dissimilar from the situation for the craze at the crack tip in continuous fracture [1] where the loaded and unloaded craze were of very similar shape, suggesting a uniform extension of material along the craze as the craze is loaded and a uniform contraction (i.e. relaxation) of material when the craze is unloaded. It should perhaps be emphasized that there was no evidence of discontinuous crack growth in these experiments, and it appeared that crack growth occurred during every cycle. Fig. 5c shows the results for a higher loading level, and in this case there is a more uniform extension of the craze on loading, although again it appears that the deformation is least near the craze tip. Another feature which these results also reveal is the hysteresis shown by the difference between the craze extensions on loading and unloading.

We have concluded from these results that in fatigue, as distinct from continuous crack growth in fracture, the stress (the so-called *craze stress*) is not constant along the length of the craze. Moreover, there can be a substantial part of the craze near the craze tip where the stress does not reach a value corresponding to the craze stress, i.e. the stress for crazing equivalent to the yield stress of the bulk polymer. There can also be hysteresis effects similar to those observed for the loading and unloading of an isolated craze by Kambour [14]. Indeed, the material near the craze tip is not being stressed to the point at which further uncrazed material will be drawn into the craze.

3.3. Craze contours

Craze geometry was measured only for a smooth growth mode. In this experiment the geometry itself does not seem to depend very much on ΔK or on the waveform. At the same ΔK repetition, the craze length and opening displacement vary over a wide range in different specimens as shown in Table I, and the geometry varies at different crack lengths of even the same specimen. When a crack has a curved front, say convex forward, the craze geometry may vary along the crack tip line, being short at the centre but long at the sides, while the crack grows keeps its craze front geometry almost the same. This implies also that the craze size does not depend very much on the growth rate, because locally different craze sizes give the same growth rate.

Fig. 6 shows the deformation of the craze fibrils at the crack tip and at the middle of the craze length, as a function of applied K during a whole cycle. As long as ΔK remains small, the crazes deform almost elastically as seen in the case of $\Delta K = 0.43\,\mathrm{MN\,m^{-3/2}}$, but with increasing

TABLE I Craze contour measurement

Stress intensity ($MN m^{-3/2}$)		Craze length R (μm)	Craze contour (μm)		Calculated original craze thickness (nm)	
K_{max}	K_{min}		$(\delta_b)_{max}$	$(\delta_b)_{min}$	g_a	g_b
0.44	0.01	40	0.87	0.45	80	214
0.47	0.04	19	0.68	0.31	37	162
0.52	0.02	26	0.81	0.37	60	178
0.68	0.02	25	0.85	0.35	58	165
0.69	0.01	19	0.86	0.33	45	145
0.84	0.03	29	1.11*	0.48	73	205
0.84	0.02	30	1.07*	0.51	75	187

*For moving crazes.

ΔK the deformation pattern begins to show hysteresis effects, as seen in the case of $\Delta K = 0.68\,MN\,m^{-3/2}$. This hysteresis behaviour of the crazes is quite similar to that observed in the isolated craze in PC by Kambour [14].

3.4. Craze deformation

We consider it instructive at this stage to introduce a modified Dugdale line-zone model for the craze, which takes into account the features indicated by the craze shape results. The Dugdale zone model can be considered as introducing a plastic zone of the shortest length required to cancel the stress singularity, with a constant high stress along the length of the zone. This can be regarded as the limiting case, and it gives the shortest craze for a given stress intensity level. We will therefore develop a model in which the stress is not constant along the craze. We also consider that it is important to take into account the finite thickness of the thin layer of bulk material from which the craze originates.

In view of the observation of considerable variations in the length of the craze for a given applied stress intensity factor, it would appear that there could be several possible craze stress distributions which would be able to cancel the stress singularity at the craze tip. The Dugdale model can be considered to be the limiting case which gives the shortest craze for a given stress intensity level, as shown in Fig. 7. However, as long as the same craze size is maintained during the crack growth, all the material along the craze must reach the craze stress at least once during the growth period. Since the craze length is usually longer than in the Dugdale model, the craze stress cannot act over the whole length of the craze at the same time.

To illustrate this argument, a simple model of craze deformation will be introduced. Assume that an elastic crack, accompanying a craze of length R, is subjected to stress intensity K and that the normal stress $\sigma(r)$ at a distance r from the crack tip, acts on the matrix boundary as shown schematically in Fig. 8; it is assumed here that no shear stress acts along the craze, because the craze fibril has almost no resistance to lateral forces. As shown in the Appendix, the elastic displacement of the craze boundary may be expressed as

$$v(r) = \frac{2}{\pi E^*}\left[(2\pi r)^{\frac{1}{2}}K - \int_0^R \sigma(s)\log\left|\frac{s^{\frac{1}{2}}+r^{\frac{1}{2}}}{s^{\frac{1}{2}}-r^{\frac{1}{2}}}\right| ds\right] \quad (1)$$

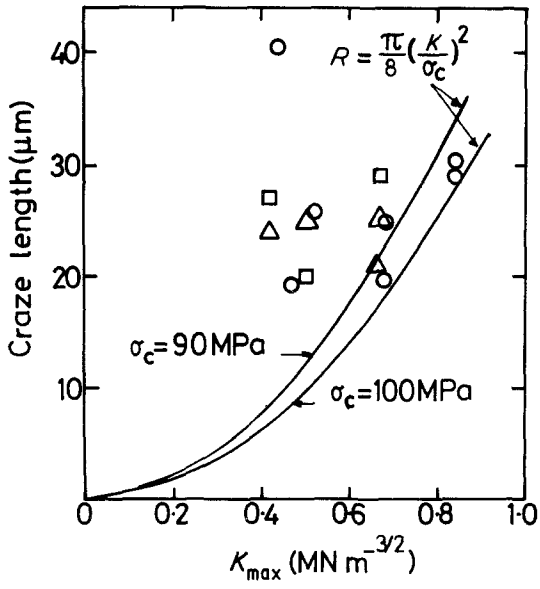

Figure 7 Measured craze length against K_{max} for symmetric triangular (○) asymmetric triangular (△) and trapezoidal waveform (□) at 0.025 Hz. Full lines show predicted relationship based on the Dugdale zone model with a constant craze stress.

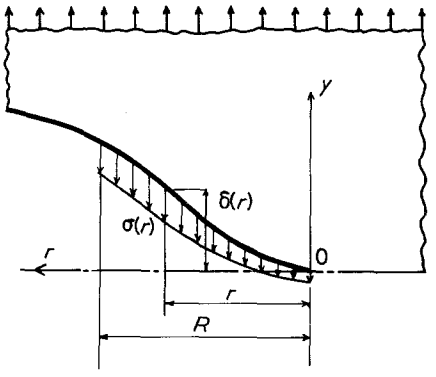

Figure 8 Craze stress acting on a craze boundary $\sigma(r)$ and a craze contour $\delta(r)$. Only the upper half is illustrated.

where E^* is the reduced Young's modulus; $E^* = E$ in plane stress and $E/(1 - \nu^2)$ in plane strain where ν is Poisson's ratio.

To cancel the stress or displacement singularity at the craze tip, K must be related to the stress distribution by

$$K = \left(\frac{2}{\pi}\right)^{\frac{1}{2}} \int_0^R \frac{\sigma(s)}{s^{\frac{1}{2}}}\, ds \qquad (2)$$

The measured craze contour $\delta(r)$ is the sum of the above elastic displacement and the original thickness of the bulk layer from which the craze was produced. Adding the original thickness $g(r)$ to Equation 1 we have

$$\delta(r) = g(r) + \frac{2}{\pi E^*} \int_0^R \left[2 \left(\frac{r}{s}\right)^{\frac{1}{2}} - \log \left| \frac{s^{\frac{1}{2}} + r^{\frac{1}{2}}}{s^{\frac{1}{2}} - r^{\frac{1}{2}}} \right| \right] \sigma(s)\, ds \qquad (3)$$

In addition, the craze fibrils which exist inside the craze contour are extended from their original length $g(r)$ to $\delta(r)$ under the stress $\sigma(r)$ acting on the ends:

$$\delta(r) = \left(\frac{\sigma(r)}{F} + \varepsilon_r + 1\right) g(r) \qquad (4)$$

where it is assumed that the craze fibril extends elastically from its relaxed strain ε_r with the modulus F as shown in Fig. 9. By eliminating $g(r)$ from the above equations, we obtain the relation between the craze contour and the stress distribution as

$$\delta(r) = \frac{2}{\pi E^*} \left(\frac{\sigma(r) + F(\varepsilon_r + 1)}{\sigma(r) + F\varepsilon_r}\right) \int_0^R \left[2 \left(\frac{r}{s}\right)^{\frac{1}{2}} - \log \left| \frac{s^{\frac{1}{2}} + r^{\frac{1}{2}}}{s^{\frac{1}{2}} - r^{\frac{1}{2}}} \right| \right] \sigma(s)\, ds \qquad (5)$$

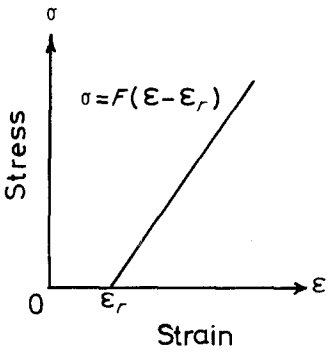

Figure 9 Stress–strain relation of already-extended craze fibrils.

For simplicity we assume the bilinear stress distribution shown in Fig. 10, which gives

$$\sigma(r) = \sigma_0 + \frac{2r}{R}(\sigma_a - \sigma_0) \qquad 0 \leqslant r \leqslant \frac{R}{2}$$

$$= \sigma_a + \frac{2}{R}\left(r - \frac{R}{2}\right)(\sigma_b - \sigma_a) \qquad \frac{R}{2} \leqslant r \leqslant R$$

We fit Equation 5 at only two points, $r = R/2$ and R. The following equations are then obtained for σ_0, σ_a and σ_b:

$$\delta_a = \frac{2R}{\pi E^*} \left(\frac{\sigma_a + F_a(\varepsilon_{ra} + 1)}{\sigma_a + F_a(\varepsilon_{ra})}\right) \left\{ \frac{3}{4} K \left(\frac{\pi}{R}\right)^{\frac{1}{2}} - \sigma_a \left[\frac{1}{2^{\frac{1}{2}}} + \tfrac{1}{2} \ln (1 + 2^{\frac{1}{2}}) \right] - \tfrac{1}{2}\sigma_b \ln (1 + 2^{\frac{1}{2}}) \right\}$$

$$\delta_b = \frac{2R}{\pi E^*} \left(\frac{\sigma_b + F_b(\varepsilon_{rb} + 1)}{\sigma_b + F_b(\varepsilon_{rb})}\right) \times \left\{ \frac{3}{8} K \frac{\pi}{R} [3(2)^{\frac{1}{2}} - \ln (1 + 2^{\frac{1}{2}})] - \sigma_a [2 - 2^{\frac{1}{2}} \ln (1 + 2^{\frac{1}{2}})] - \tfrac{1}{2}\sigma_b \left[1 + \frac{1}{2^{\frac{1}{2}}} \ln (1 + 2^{\frac{1}{2}}) \right] \right\}$$

$$\sigma_0 = \tfrac{3}{4} K \left(\frac{\pi}{R}\right)^{\frac{1}{2}} - 2(2^{\frac{1}{2}} - 1)\sigma_a - \tfrac{1}{2}(2 - 2^{\frac{1}{2}})\sigma_b$$

where the suffices 0, a and b correspond to the points $r = 0$, $R/2$ and R respectively.

3.5. The stress field along the craze

By fitting the measured craze geometry to the above equation, the bilinear stress distribution

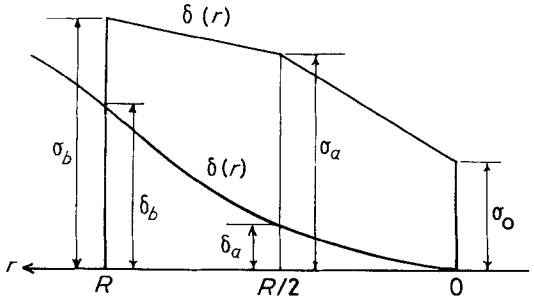

Figure 10 Bilinear distribution of the craze stress and the measured craze contour. 0, *a* and *b* refer to the points at the craze tip, at the middle, and at the crack tip respectively.

along the craze boundary was calculated. It was found that a combination of $F = 60$ MPa and $\varepsilon_r = 2$ gave the best fit to the craze deformation behaviour. A value of Young's modulus $E = 2.8$ GPa and Poisson's ratio $\nu = 0.3$ were also used. Fig. 11 shows the calculated stress distribution along the craze at the maximum load. It can be seen that the stress distribution is somewhat uneven, with the highest stresses at the crack tip. Even at the same stress intensity level, the longer the craze, the lower the stress falls at

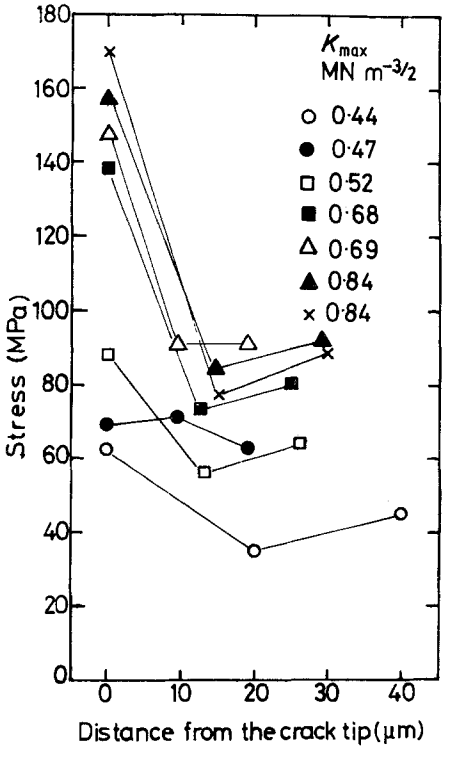

Figure 11 Calculated craze stress distributions along crazes of various lengths at maximum stress intensities.

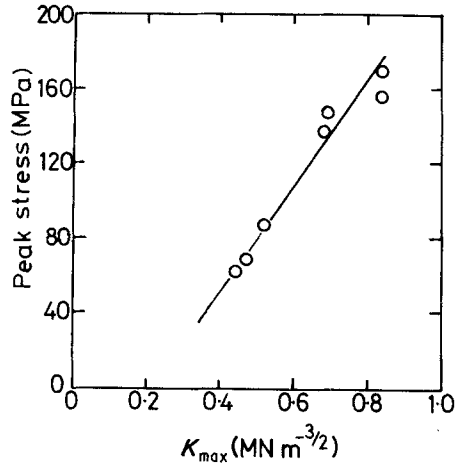

Figure 12 Peak stress attained at the crack tip against applied maximum stress intensity K_{max}.

points far from the crack tip. The peak stress at the crack tip σ_b correlates well with the applied K_{max} independent of the craze length as shown in Fig. 12, a result which is similar to that of the simple Dugdale model [10].

Table I also shows the calculated original thickness of crazes at the crack tip g_b and at the middle of the craze g_a. The original thickness does not depend on the applied K level, but correlates with the craze length as shown in Fig. 13. This implies that the craze grows longer and thicker by consuming more original bulk material which turns into craze fibrils. Consequently the strain of the craze fibrils, especially

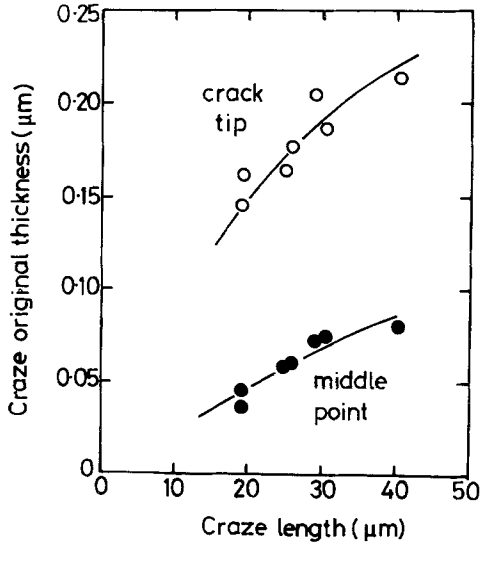

Figure 13 Calculated original thickness of craze against craze length.

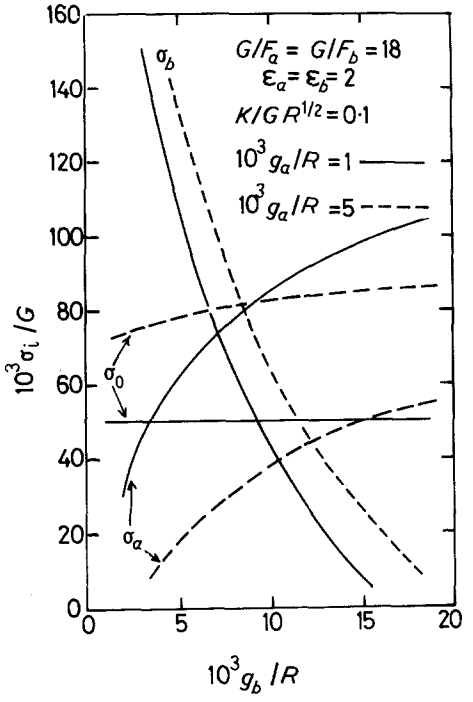

Figure 14 Variation of craze stresses σ_0, σ_a, σ_b as a function of the original thickness of the craze g_a and g_b at load level $K/GR^{\frac{1}{2}} = 0.1$. 0, a and b refer to the points at the craze tip, at the middle, and at the crack tip, respectively. Other constants used in the calculation are shown in the diagram.

at the crack tip, remains almost the same for a given stress intensity level regardless of craze size, and the stress state achieved is proportional to K. Unless the applied stress intensity level is very high, the original thickness is thought not to change very much during a fatigue cycle, and hence it describes the whole deformation behaviour of the craze contour. The solid lines in Fig. 6 show the predicted deformation, which corresponds well with the experimental data.

3.6. Craze and crack growth mechanisms

The original craze thickness also determines the stress field around the craze. Fig. 14 shows how the stress changes with g_a and g_b at a constant load level $K/GR^{\frac{1}{2}} = 0.1$. The stress states are illustrated in Fig. 15 for exaggerated combinations of g_a and g_b, although the actual situation would involve much narrower ranges of g_a and g_b. While g_b/R remains small, the stress at the crack tip becomes highest as shown in Fig. 15a. In this case, at some load level the matrix wall at this point will be drawn into craze fibrils making g_b thicker, or possibly craze fibrils at this point may break resulting in crack growth. In the former case the original thickness of the craze increases, to give (say) $10^3 g_b/R = 10$, and stress redistribution occurs to produce the situation represented in Fig. 15b where the stress at the middle point of the craze becomes the highest. An increase of g_a may then occur and lead to the stress state shown in Fig. 15c, where the craze tip is subjected to the highest stress. The craze will then grow in length, and finally the situation will return to that of Fig. 15a due to the decrease of g_a/R and g_b/R. It is considered that the above sequence of events may be completed within one fatigue cycle or during several cycles, depending on the applied K level.

It is also to be noted that newly fibrillated crazes may exhibit a large hysteresis in their cyclic stress–strain behaviour, in the same manner as the completely relaxed craze [14]. The stress state in the re-loading period is therefore no longer the same as that in the previous unloading period at the same K level. This explains why the fatigue crack grows differently from a crack propagating under continuous loading. When the applied K is decreased to a level where

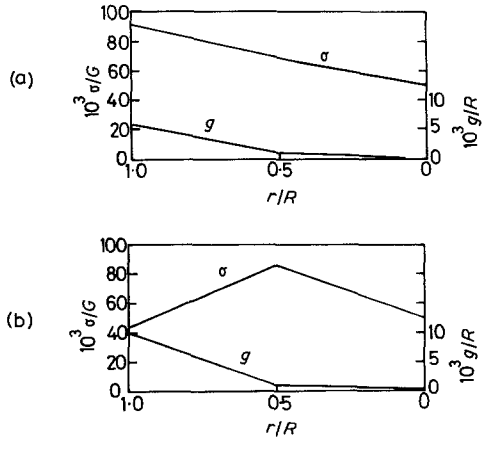

Figure 15 Typical examples of the craze stress distribution with changing original thickness of the craze: (a) $10^3 g_a/R = 1$, $10^3 g_b/R = 6$; (b) $10^3 g_a/R = 1$, $10^3 g_b/R = 10$; (c) $10^3 g_a/R = 5$, $10^3 g_b/R = 10$.

no additional fibrillation occurs on the craze boundary, the craze deformation becomes elastic and load cycling cannot cause any craze growth and crack growth. This will correspond to the lower bound of crack growth.

4. Conclusions

1. Two fatigue fracture modes are observed: smooth fracture surfaces and rough surfaces. The appearance of a plateau in the plot of crack growth rate against ΔK may be caused by the transition from the former mode to the latter. The latter gives slower growth rate than the former.

2. Very great scatter in craze length and craze thickness are observed at the maximum load. Hence the simple Dugdale model is not adequate to explain craze deformation during the fatigue cycle. By taking into account the craze fibril deformation as well as the deformation of the craze contour, a simple craze deformation model was constructed which gives a good fit to the experimentally observed deformation behaviour.

3. The large variation in craze size is attributed to variation of the original craze thickness; the original thickness grows with craze length. However, no matter how long the craze is, calculated stresses at the crack tip become almost the same at the same K. This may be the reason why no cyclic rate dependence, and no waveform dependence, are observed in the crack growth rate.

Appendix

When a pair of concentrated forces P are applied at the edge of a semi-infinite crack as shown in Fig. A1, the Westergaard stress function is given by

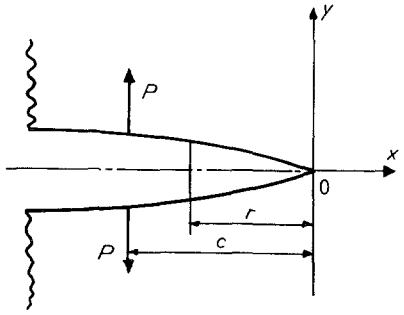

Figure A1 A pair of concentrated forces acting at the edges of a semi-infinite crack.

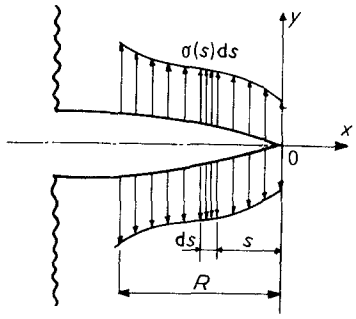

Figure A2 Distributed forces acting along the edges of a semi-infinite crack.

$$Z = \frac{1}{\pi(z + c)}\left(\frac{c}{3}\right)^{\frac{1}{2}} P$$

where $z = x + iy$. From this the crack edge displacement in the y direction is calculated as

$$v = \frac{2}{\pi E^*} P \log \left| \frac{c^{\frac{1}{2}} + r^{\frac{1}{2}}}{c^{\frac{1}{2}} - r^{\frac{1}{2}}} \right|$$

and the stress intensity factor for this situation is

$$K = \left(\frac{2}{\pi c}\right)^{\frac{1}{2}} P$$

In the case of $c \gg r$, the log term can be approximated to

$$\log \left| \frac{c^{\frac{1}{2}} + r^{\frac{1}{2}}}{c^{\frac{1}{2}} - r^{\frac{1}{2}}} \right| \simeq 2\left(\frac{r}{c}\right)^{\frac{1}{2}}$$

and the displacement is expressed using K as

$$v = \frac{2}{\pi E^*} (2\pi r)^{\frac{1}{2}} K$$

On the other hand, when the forces are distributed along some distance R as in Fig. A2 then

$$v = \frac{2}{\pi E^*} \int_0^R f(s) \log \left| \frac{s^{\frac{1}{2}} + r^{\frac{1}{2}}}{s^{\frac{1}{2}} - r^{\frac{1}{2}}} \right| \mathrm{d}s$$

and

$$K = \left(\frac{2}{\pi}\right)^{\frac{1}{2}} \int_0^R \frac{f(s)}{s^{\frac{1}{2}}} \mathrm{d}s$$

where $f(s)$ is a distribution function of the force along the crack edge.

Acknowledgements

We wish to thank the Yoshida Science Foundation for providing financial support to Y. Imai. We also wish to thank Mr B. Eadon for making the fatigue loading equipment, and

Dr N. H. Ladizesky for advice on photographic techniques.

References

1. H. R. BROWN and I. M. WARD, *Polymer* **14** (1973) 469.
2. G. P. MORGAN and I. M. WARD, *ibid.* **18** (1977) 87.
3. W. DÖLL, L. KONCZOLL and M. G. SCHINKER, *ibid.* **24** (1983) 1213.
4. W. DÖLL, "Advances in Polymer Science", edited by H. H. Kausch (Springer-Verlag, Berlin, 1983) p. 105.
5. M. J. DOYLE and J. G. WAGNER, "Toughness and Brittleness of Plastics", edited by R. D. Deanin and A. M. Cragnola (American Chemical Society, New York, 1976) p. 63.
6. S. J. ISRAEL, E. L. THOMAS and W. W. GERBERICH, *J. Mater. Sci.* **14** (1979) 2128.
7. *Idem, ibid.* **15** (1980) 2994.
8. L. KONCZOLL, M. G. SCHINKER and W. DÖLL, "Fatigue in Polymers" (Plastic and Rubber Institute, London, 1983) 4.1.
9. J. S. HARRIS and I. M. WARD, *J. Mater. Sci.* **8** (1973) 1655.
10. D. S. DUGDALE, *J. Mech. Phys. Solids* **8** (1960) 100.
11. R. W. HERTZBERG and J. A. MANSON, "Fatigue of Engineering Plastics" (Academic Press, New York, 1980) p. 160.
12. B. GROSS and J. E. SRAWLEY, Technical Note D-3295, NASA (1966).
13. J. S. BRODERICK, R. A. DUCKETT and I. M. WARD, "Fatigue in Polymers" (Plastic and Rubber Institute, London, 1983) 5.1.
14. R. P. KAMBOUR and R. W. KOPP, General Electric Company, Schnectady, USA, Technical Information Series No. 67-C-374 (1967).

Received 8 August
and accepted 10 September 1984